



## Investigation of bonding strength and sealing behavior of aluminum/stainless steel bonded at room temperature

M.M.R. Howlader<sup>a,\*</sup>, T. Kaga<sup>b</sup>, T. Suga<sup>c</sup>

<sup>a</sup>Electrical and Computer Engineering Department, McMaster University, 1280 Main Street West, Hamilton, ON, Canada L8S 4K1

<sup>b</sup>Research Institute of Industrial Product, Gifu Prefecture, Gifu, Japan

<sup>c</sup>Research Center for Advanced Science and Technology, The University of Tokyo, 4-6-1 Komaba, Meguro-ku, Tokyo 153-8904, Japan

### ARTICLE INFO

#### Article history:

Received 25 June 2009

Received in revised form

26 February 2010

Accepted 28 February 2010

#### Keywords:

Surface activated bonding

Surface roughness

Impurity

Bonding strength

Leak rate

UHV component

### ABSTRACT

This article reports the direct bonding of aluminum (Al) [99.999% (5N), 99% (2N)] and stainless steel SUS (304, 316) without heating for sealing in the ultra high vacuum (UHV) components. For bonding, the smooth surfaces of the Al and SUS specimens were activated using argon fast atom beam (Ar-FAB) for 1–60 and 60 min, respectively, in a background pressure of  $6.0 \times 10^{-5}$  Pa followed by close contact under an external pressure of 960 N. High bonding strength resulted in the bonded mates of Al and SUS304 activated for 30 and 60 min, respectively, due to the adhesion forces of the surface atoms. Tensile pulling tests showed bulk fractures in Al with impurity dependent bonding strength. The bonding strengths for the Al5N/SUS304 and Al2N/SUS304 specimens were higher than 60 and 100 MPa, respectively. For the sealing test, the smooth surface of the SUS316 flange containing a hole was bonded with Al after surface activation 60 and 30 min, respectively. Leak rates for Al5N/SUS316 and Al2N/SUS316 specimens were  $1.5 \times 10^{-11}$  and  $2.0 \times 10^{-11}$  Pa m<sup>3</sup>/s, respectively. These results satisfy the permissible leakage of a large-sized UHV chamber. Time dependence of the leak test behavior for both specimens shows a stable leak rate. Therefore, the sealing of Al/SUS316 may be utilized for the fabrication of corrosion free joints for fluid flow in the cooling of electron guns of small size equipment such as portable scanning electron microscopes in UHV pressure.

© 2010 Elsevier Ltd. All rights reserved.

### 1. Introduction

Direct bonding of dissimilar materials may provide corrosion resistant and highly conductive bonded interfaces. Such bonded interfaces may require producing miniaturized joints for light-weight and portable technological applications [1–5]. For example, for electron gun cooling such miniaturized joints may be required to permit fluid flow in a portable scanning electron microscope [1]. The joints may be corroded unless the joints do not have protrusions/layers that do not react with the fluid. The joints may also need to be sustained in ultra high vacuum (UHV) pressure for such applications. Generally, the bonding processes for two or more solid-state materials can be categorized into adhesive bonding [2], spark welding [3], explosive bonding [4], and diffusion bonding [5,6]. However, the processing for a certain combination of dissimilar joined metals produces excessive brittle intermetallic compounds that degrade the bonded interface [6,7]. The solid-state

bonding technologies without such undesirable diffusion and reaction layer at the interfaces are important for the joining of dissimilar metals. The joining of aluminum to stainless steel (SUS) has been reported by the solid-state bonding methods such as diffusion bonding [5,6], friction welding [7–11], vacuum roll bonding [12] and hot roll bonding [13]. Current bonding technologies for Al/SUS produce brittle intermetallic compounds in the range of few nanometers [14] to a few hundred micrometers [6] at the interface. The thinner the intermetallic phase, the better the bonding strength [15]. Therefore, there is a demand for bonding technologies that can be used for the fabrication of a bonded interface without intermetallic compounds.

A room temperature solid-state bonding process with an atomic-scale bonding resolution, called surface activated bonding (SAB), has been developed for such purposes [14,16]. This process joins two smooth sputter cleaned surfaces with the use of energetic sources such as argon fast atom beam (Ar-FAB) and low energy ion beam in UHV. The sputter cleaning allows the removal of native oxides, carbon contaminants and atmospheric particles from the surface, which is known as the activated surface. The contact of the activated surfaces results in strong adhesion due to the attractive

\* Corresponding author.

E-mail address: [mrhowlader@ece.mcmaster.ca](mailto:mrhowlader@ece.mcmaster.ca) (M.M.R. Howlader).

forces of the surface atoms. Therefore, the bonded interface fabricated by the SAB may be better than that of the other joining processes, such as friction welding, because of the absence of oxides on the mated surface during bonding. The absence of these oxides may reduce extended corrosion at the joint. This method does not require pre- and post-bonding heating treatments for the bonding of a diverse combination of materials. Also, the SAB does not produce any significant intermetallic compound at the interfaces.

One of the key requirements for the SAB is the smooth surface with roughness (in root mean square) of less than 1 nm for the mated materials [16]. While such surface roughness of semiconductor materials can easily be achieved, the surface roughness of metals is difficult to obtain. The amount of doping in the materials may significantly control the surface roughness. If the metal were an alloy, it would have higher surface roughness than even that of metal because of the presence of different grains with different hardnesses [9]. However, the role of impurities in aluminum on the surface roughness of the activated surface as well as its relationship with the bonding strength has not yet been discovered.

While the welding and brazing are generally being used for solid-state metal/metal joints for vacuum tightness of vacuum tools and devices [17], the room temperature hermetic joining of Al and SUS would give new opportunities for vacuum tight applications in the UHV components. Although the hermetic sealing behavior of the glass/silicon cavities prepared by bonding of silicon patterns with glass wafers using SAB has been examined by placing a cantilever in the cavity before bonding followed by measurement of the quality factor of the cavity with use of the atomic force microscope (AFM) principle [18], the airtight sealing between Al and SUS has not yet been investigated.

In this study, the authors investigated the role of impurities of aluminum on the room temperature bonding of Al/SUS using surface activated bonding with the influence of activation parameters on the bonding strength. The leakage behavior of the Al/SUS joint was also investigated for the sealing applications in the ultra high vacuum components.

## 2. Experimental procedure

### 2.1. Specimen preparation

Stainless steel plates (SUS304) of (10 × 20 × 0.8) mm and aluminum rods (Al) [99.999% (5 N), 99% (2 N)] were used for bonding experiments. Commercially available standard SUS316 flanges of 34 mm in diameter and 2 mm thick bonded with Al2N

and Al5N were used for the ultra high vacuum (UHV) leak test. A hole of a diameter of 1 mm was made at the center of the SUS316 flange. The Al rod 20 mm in length and 10 mm in diameter with a hemispherical surface of radius of 25 mm (Fig. 1) was used. Tables 1 and 2 show the chemical compositions for SUS and Al, respectively, used for the bonding. The Al5N specimen has 99.999% purity. The Al2N has silicon and iron impurities with concentrations of 0.03% and 0.17%, respectively. After iron, the major elements in the both types of steels (i.e., SUS304 and SUS316) are chromium and nickel. These elements have 2–4% discrepancies. Another difference in the SUS304 and SUS316 is the 2–3% molybdenum, which is only present in SUS316 specimen.

Both the SUS304 plate and SUS316 flange surfaces were polished by water proof silicon carbide polishing paper up to # 2400 (12 μm). The polished surfaces with abrasive papers were further polished by 9 and 3 μm diamond powder followed by a final polishing using colloidal silica suspension of 0.04 μm. On the other hand, the hemispherical surface of Al rods was polished using carbide abrasive paper followed by polishing with different grades of alumina powder. The polishing was completed after treating with 0.1 μm of alumina powder. The Al specimens were annealed at 773 K for 120 min in a vacuum pressure of  $7.0 \times 10^{-4}$  Pa. The specimens were electrolytically polished in a mixture of perchloric acid (60%) and ethanol of ratio 3:7 for 10 min. The applied voltage and current during electrolytic polishing were 15 V and 3 A.

### 2.2. Bonding tool and experiment

Fig. 2 shows the schematic diagram of the SAB tool used for the bonding experiments. This is single chambered bonding equipment with high vacuum pressure, which is positioned with two Ar-FAB sources. They were placed at 45 deg with respect to the top and bottom specimens. The specimens were cleaned using the sputter cleaning Ar-FAB sources of 1.5 kV and 15 mA in a high vacuum pressure of  $4.0 \times 10^{-5}$  Pa. The surface activation time for the Al specimens was in the range from 1 to 60 min, and for SUS304 was fixed for 60 min unless otherwise mentioned. For leak test experiments, the activation time was 60 min for both the specimens. The etching rate (measured by Tenkor surface profiler) for Al5N and SUS304 was 1.3 and 0.9 nm/min, respectively.

The bottom specimen with the holder was fixed with the lower stage. The top specimen with the holder was flipped over and fixed with the bonding head. The bonding head with the top specimen was moved downward under a contact pressure until reaches to 960 N, which was held for 3 min.

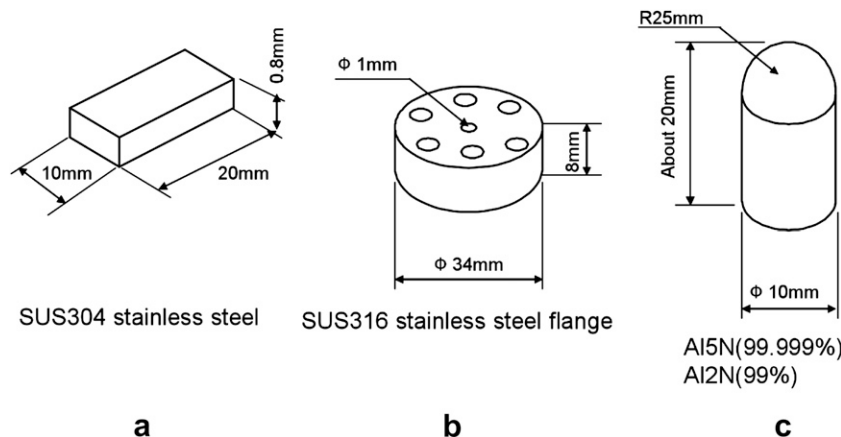


Fig. 1. Geometrics of the specimens used for the bonding experiments. (a) SUS304 stainless steel plate, (b) SUS316 stainless steel flange, (c) Al5N, Al2N.

**Table 1**  
Chemical compositions of stainless steel

	Composition (wt%)					
	Cr	Ni	Si	Mn	C	Mo
SUS304	18–20	8–11	<1	<2	<0.08	–
SUS316	16–18	10–14	<1.5	<2	<0.08	2–3

### 2.3. Tensile pulling test and sealing characterization

After bonding, the tensile strength was measured using a tensile pulling test machine. A tensile pulling tester (AGS-1 kNG) from Shimadzu Corporation was used for the tensile strength measurements of the bonded interface. In order to perform the tensile test, a hole was prepared across the one-third of the Al specimen from the top of the bonded specimen (which is the opposite side from the bonded side). The hole of the bonded specimen was aligned to the holes of the clamps at the upper stage of the tensile tester and a stainless steel rod was inserted to the holes from the edge of the clamps to hold the top side of the bonded specimen. For holding the bottom side of the bonded specimen, the SUS304 plate was mechanically held by the specimen fixture at the bottom stage of the tester. For tensile test, the bottom stage was kept rigid, while the upper stage was moved by the computer control to pull the bonded specimen perpendicularly to the bonded interface. Tensile pulling tests were done at a speed of 1 mm/min.

The vacuum sealing behavior was measured using a helium leak detector (Pfeiffer Vacuum, HTL 260). The details of the measurement for the leak rate of Al/SUS are described in Section 3.3.

## 3. Results and discussion

### 3.1. Surface chemistries and roughness

The Al and SUS304 surfaces have been analyzed by X-ray photoelectron spectroscopy (XPS) using Ar-FAB before and after irradiation to insight the surface condition. Fig. 3a shows XPS spectra of the Al5N surface before and after 10 min Ar-FAB irradiation. The XPS experiments were done with another bonding tool equipped with the similar Ar-FAB used for the sputter cleaning, and XPS [16]. After sputter cleaning with the Ar-FAB sources, the XPS spectra were taken without exposure to air. Upper and lower spectra represent the surface condition before and after irradiation, respectively. The peaks for native oxides and carbon were observed on electrolytically cleaned Al surface. The oxygen and carbon from the Al surfaces can be removed using sputter cleaning with the Ar-FAB. The sputter cleaning for 10 min completely removed the oxygen and carbon from the Al surface, which is called the activated surface. The sputter cleaning time required for the cleaning of the SUS304 surface was higher than that of the Al surface. The XPS spectra for the activated and non-activated SUS304 stainless steel surface are shown in Fig. 3b. The sputter cleaning for surface activation is done for 45 and 60 min. While the sputter cleaning for 60 min completely removed the carbon and oxygen from the SUS304 surface, the carbon and oxide remained on the surface activated for 45 min.

**Table 2**  
Chemical compositions of aluminum

	Composition (wt%)		
	Al	Si	Fe
Al5N	99.999	–	–
Al2N	99	0.03	0.17

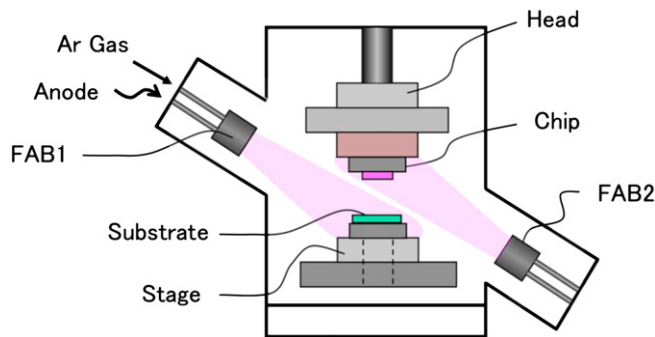


**Fig. 2.** Schematic diagram of a surface activated bonding (SAB) tool.

Surface roughness of the mating pairs along with the surface activation controls the bonding outcome in the SAB method [16]. This is because strong adhesion in the SAB develops only while a smooth surface provides close contact between the activated surfaces. The surface roughness of Al and SUS specimens was investigated using an AFM from Seiko Instruments. As previously described, the flat surfaces of Al were prepared for surface roughness measurements by mechanical polishing and chemical cleaning

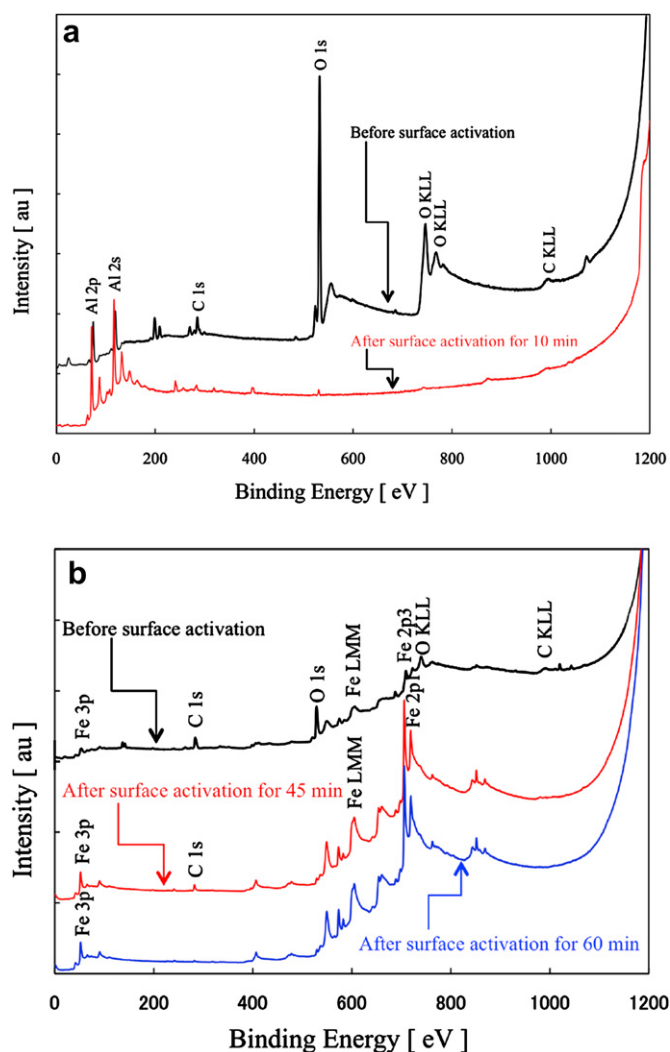


**Fig. 3.** XPS spectra of (a) Al5N and (b) SUS304 surface before and after FAB irradiation. The sputter cleaning time for Al and SUS304 by the Ar-FAB irradiation was 10 and 60 min, respectively, to remove carbon and oxygen.

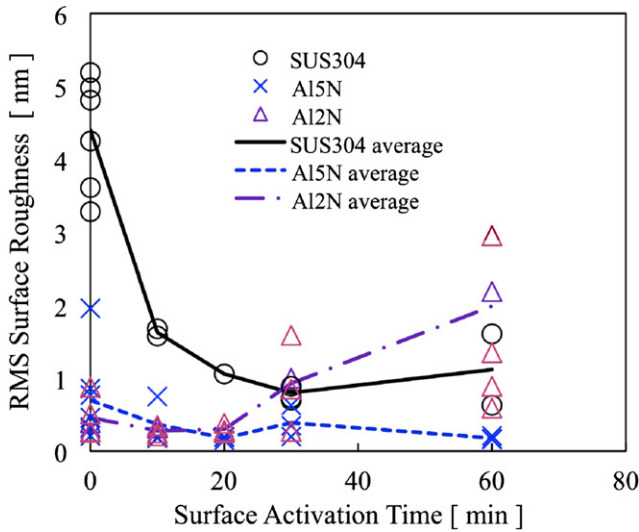


Fig. 4. Surface activation time dependence of Ar-FAB on the surface roughness of Al2N, Al5N and SUS304. The scanning area used for the AFM measurements was  $3 \times 3 \mu\text{m}^2$ .

processes. Fig. 4 shows the sputter cleaning time dependence of the surface roughness for Al2N, Al5N, and SUS304 specimens. The root mean square (rms) values of the surface roughness for the SUS304, Al5N and Al2N specimens were 1.3, 1.3, and 2.9 nm, respectively. The surface roughness for Al5N remains constant with the increase of the sputter cleaning time. In Al2N, the surface roughness decreases up to 20 min cleaning, and then significantly increases with the increase of the sputter cleaning time. The surface becomes rough with the increase of sputter cleaning time, which may be due to the etching rate difference of Al itself. Also, the impurity may have strong influence on it. The surface roughness of SUS316 flange could not be observed because the flange was not accommodated in the AFM specimen cell. However, the surface roughness of the

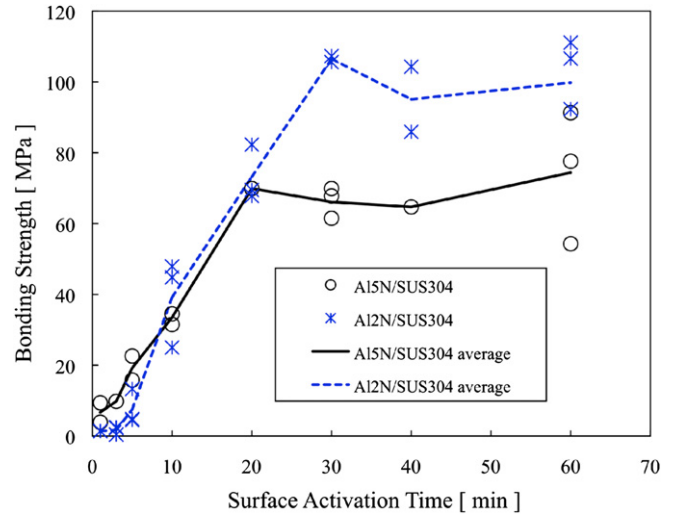


Fig. 5. The bonding strength of Al/SUS304 as a function of surface activation time of Al. The surface activation time for SUS304 was kept constant for 60 min.

flange is likely identical to that of the SUS304 specimen because of the identical polishing conditions.

### 3.2. Bonding strength and mechanism

Fig. 5 shows the surface activation time dependence on the bonding strength of Al5N/SUS304 and Al2N/SUS304 specimens. The surface activation time for SUS was 60 min. Bonding strength increases with the increase of the surface activation time up to 20 and 30 min, respectively, for Al5N and Al2N, and then it changes monotonously as a function of sputter cleaning time. While the Al5N specimens were bonded at low activation time, even lower than 3 min, the Al2N specimens were not bonded without cleaning for a minimum of 5 min. As previously seen from the XPS spectra that the carbon contaminants are present on Al (both 2 and 5 N) and SUS

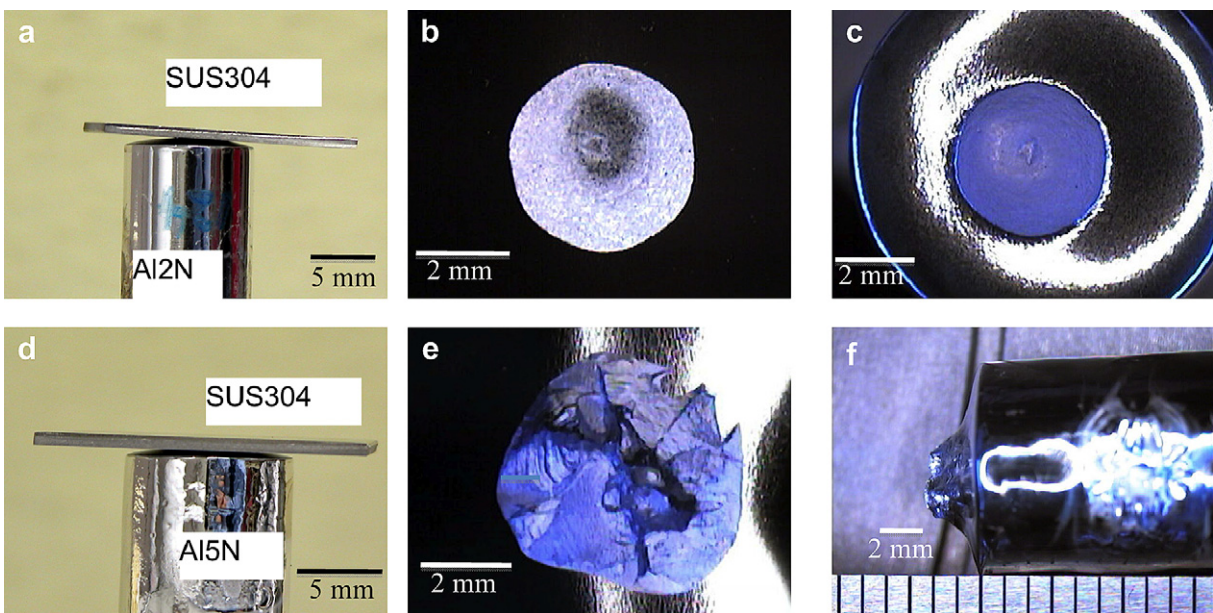
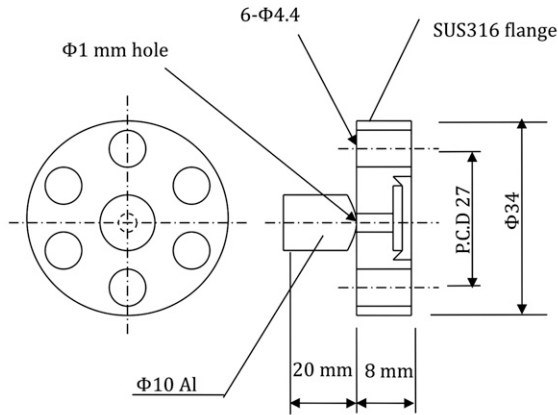
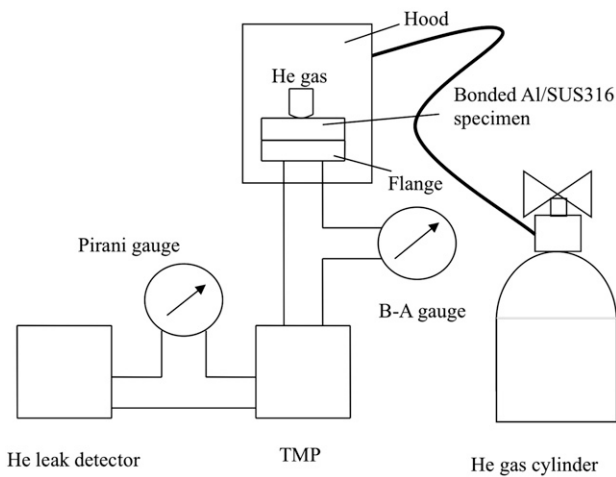


Fig. 6. Optical micrographs of (a) Al2N/SUS304 before tensile pulling test, (b) SUS304 side of the interface of Al2N/SUS304 after tensile pulling test, (c) Al2N side of interface of Al2N/SUS304 after tensile pulling test, (d) Al5N/SUS304 before tensile pulling test, (e) SUS304 side of the interface of Al5N/SUS304 after tensile pulling test and (f) Al5N side of interface of Al5N/SUS304 after tensile pulling test. The specimens were not separated at the interface and Al5N was elongated. Al was broken in the bulk.



**a** Geometries of sealed flange



**b** Diagram for leak test setup

**Fig. 7.** Schematics of (a) sealed flange and (b) leak test setup.

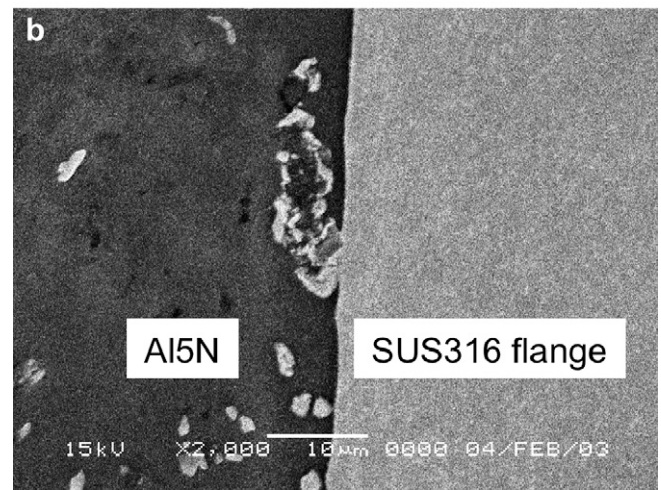
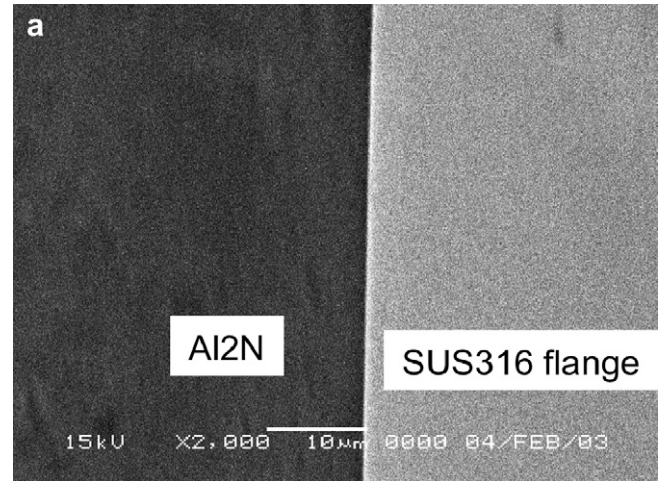


**Fig. 9.** Scanning electron microscope (SEM) photographs for the cross section of (a) Al2N/SUS316 flange and (b) Al5N/SUS316 flange. These photographs showed no pinholes and cracks across the interface.

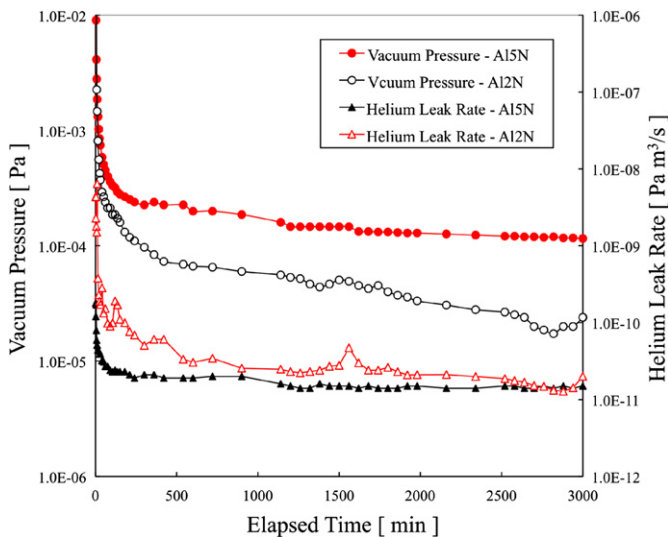


**Fig. 8.** Results of the leak test of Al5N/SUS316 flange and Al2N/SUS316 flange for 50 h. The stable leak rate is sustainable for UHV pressure.

surfaces activated for less than 10 and 60 min, respectively. This indicates that the imperfectly activated Al is bonded with perfectly activated SUS304. But after tensile pulling test, the rupture occurs at the bonded interface for the specimen activated for less than 20 min because of the low bonding strength. This is caused by the presence of carbon and oxygen on the imperfectly activated surfaces. For activation time over 20 min for the Al5N/SUS304 and 30 min for the Al2N/SUS304 the breaking occurs at 60 MPa for the first one and around 110 MPa for the second one. Note that the surface activation time for SUS304 was 60 min. The bonding strengths correspond to the bulk strengths of the two aluminum specimens. After surface activations of Al2N and Al5N for 30 min, the bonding strengths of Al2N/SUS304 are higher than that of Al5N/SUS304. The reduction of bonding strength can be presumably attributed to higher deformation (under identical bonding force) and higher elongation (after tensile pulling) of Al5N than that of Al2N. The differences in the bonding strength could come from microstructural defects in the aluminum induced by the preparation of the specimens (such as inhomogeneous Al hemispherical shapes fabricated by hand polishing and electrolytic polishing effects on hemispherical surfaces of Al) and their impurity. Also, an insignificant influence on the bonding strength could result from artifacts caused by the jig setting during tensile pulling test.

In order to observe if the perfectly activated specimen (i.e., 60 min) could withstand higher stress, a smaller hole was made on

the backside of Al specimen parallel to the SUS304 specimen. The bonding strengths for the Al5N/SUS304 specimens activated both for 60 min vary between  $\sim 80$  and 90 MPa. The tensile pulling tests were not stopped until the Al5N side was broken. The Al5N specimen elongated, but not separated at the interface (Fig. 6c). Fig. 6a–c shows the optical images of bonded Al2N/SUS304, debonded SUS304 and debonded Al surfaces, respectively. Fig. 6d–f shows the optical images of bonded Al5N/SUS304, debonded SUS304 and debonded Al surfaces, respectively. A remarkable difference in the bonding areas for the Al5N/SUS304 and Al2N/SUS304 is observed, which is due to the difference in the hardness dependent deformation of Al2N and Al5N (figs. 6c and f). The estimated average bonding areas of the specimens after debonding are 12.17 and 22.26 mm<sup>2</sup>, respectively. The higher debonded area of Al5N than that of Al2N is due to its higher deformation caused by higher purity. The higher the purity, the lower the hardness of the materials. The hardnesses of Al2N and Al5N were measured using a dynamic ultra-micro hardness tester (DUH-W201) from Shimadzu Corporation. The hardness was 32.2 and 28.7 HV (vicars hardness) for Al2N and Al5N, respectively. The impurity dependent higher deformation is consistent with the hardness values of Al. In both the Al2N/SUS304 and Al5N/SUS304, bulk fractured Al remained on SUS304 side, again because the Al specimen is weaker than the SUS304 specimen (Fig. 6b, c, e and f). However, the only difference is the height of Al fracture left on the SUS304 side, which corresponds to the difference in elongation of Al2N and Al5N.

### 3.3. Leak test

To evaluate the application feasibility of the interface of Al bonded with SUS flange for vacuum tightness application in the UHV pressure, the leakage behavior of the interface was performed. As mentioned previously, a hole of 1 mm diameter was made at the center of the SUS316 flange. The Al5N to SUS316 flange and Al2N to SUS316 flange were both bonded for seal tests. Fig. 7 (a) shows the schematic geometry for the bonded flange. The Al and SUS316 specimens were bonded after surface activation for 30 and 60 min, respectively, under an external pressure of 960 N. Before surface activation, the specimens were manually aligned and placed in the chamber for surface activation and bonding. The manual alignment resulted in misalignment between the center of the holed flange and Al. The specimens were separated by pulling test and the sealing width was measured. The lowest sealed widths obtained were 1.2 and 0.9 mm, respectively, for Al5N/SUS316 and Al2N/SUS316.

Fig. 7 (b) shows the schematic diagram for the experimental setup used for the leak test. The flange side of the bonded specimens was tightly connected to a port of a vacuum chamber through a Cu gascade using nuts and bolts. Then the chamber was connected with the Al/SUS316 flange specimens and placed in a vinyl hood filled with the He gas. As soon as the pumping system started to vacuum the chamber, the vacuum pressure and the leak rate of the chamber were monitored. The vacuum pressure was monitored from the pressure gauge located between the TMP and the test chamber. The leak rate was taken directly from the reading of the He leak detector. If there were leakage at the sealed interface between Al/SUS316 flange, the leak detector would then detect He gas entering to the vacuum chamber.

Fig. 8 shows the time dependence as a function of vacuum pressure and He leak rate of Al5N/SUS316 and Al2N/SUS316. The estimated leak rates were  $1.5 \times 10^{-11}$  and  $2.0 \times 10^{-11}$  Pa m<sup>3</sup>/s, respectively after 50 h of testing. Time dependency of the leak rate behavior showed stable and constant vacuum pressure that is sustainable to UHV pressure. The vacuum pressure and leak rate became stable within 50 min. These values satisfied the equivalent permissible leakage of the large size UHV chamber [17].

### 3.4. Microstructural observation

Since the authors have already confirmed the presence of a few nm amorphous layers at the Al/SUS bonded interface created by the SAB [14], the interfacial microstructure over a wide area was focused using a scanning electron microscope (SEM) in order to observe interfacial defects at the interface that might influence on the leakage. In general, the cleaning of surfaces with energetic particles generates defects, such as pinholes and cracks, which can obstruct to maintain the low leak rate. Fig. 9a and b shows the SEM photograph of a cross section of the Al2N/SUS316 flange and Al5N/SUS316 flange, respectively. The images do not show either amorphous layer (within this low resolution) or pinhole or crack across in the interface. Due to the absence of the pinhole and crack, the leak rates for the bonded specimens were very low. Bonding strength associated with the vacuum tightness of the Al/SUS interface may indicate considerable application in UHV tools, and automobiles especially in the metallic multi-channels [1,19] with chemicals and other fluids where corrosion could be a significant problem.

## 4. Conclusions

The smooth surfaces of Al5N, Al2N and SUS304 have been bonded after sputter cleaning using Ar-fast atom beam in UHV at room temperature. During bonding, an external force of 940 N was used. The XPS study shows that the surface activation of Al (2 and 5 N) and SUS for 10 and 60 min, respectively, removes the surface oxides and carbon contaminants. The bonding strength of the specimens activated above 20 min for the Al2N, 30 min for the Al2N and 60 min for the SUS304 are fractured in the bulk Al but not in the interface. Both the bonded specimens of Al5N/SUS304 and Al2N/SUS304 have bonding strength higher than 60 MPa, which were not separated at the interface but broken in the bulk of Al. The impurity dependent surface roughness and bonding strength were observed. The SUS316 flange with a hole was bonded with Al (2 and 5 N) for the investigation of sealing behavior of the Al/SUS316 after surface activation for 60 and 30 min, respectively. Leak rates of  $1.5 \times 10^{-11}$  and  $2.0 \times 10^{-11}$  Pa m<sup>3</sup>/s were obtained for the Al5N/SUS316 flange and Al2N/SUS316 flange, respectively, which satisfy the permissible equivalent leakage of the large-sized ultra high vacuum chamber. Experiments for the time dependent leak test for both specimens showed that the leak rate was stable and able to sustain UHV pressure. Therefore, the bonding of Al/SUS may be used in sealing for UHV using SAB method.

## References

- [1] Miyoshi M, Okumura K, Awata S, Okada Y, Maeda T, Yamaguchi H, et al. Miniaturized finger-size electron-beam column with ceramic-type lenses for scanning electron microscopy. *J Vac Sci Technol B* 2004;22(6): 3528–33.
- [2] Zadpoor AA, Sinke J, Benedictus R. The mechanical behavior of adhesively bonded tailor-made blanks. *Int J Adhesion Adhesives* 2009;29:558–71.
- [3] Nakamura T, Hayakawa K, Tanaka S, Imaizumi H, Nakagawa Y. Bonding characteristics of various metals by DC pulse resistance heat pressure welding. *Mater Trans* 2005;46(2):292–7.
- [4] Bhalla AK, Williams JD. Production of stainless steel wire-reinforced aluminum composite sheet by explosive compaction. *J Mater Sci* 1977; 12:522–30.
- [5] Kundu S, Chatterjee S. Diffusion bonding between commercially pure titanium and micro-duplex stainless steel. *Mater Sci Eng A* 2008;480:316–22.
- [6] Bhanumurthy K, Fotedar RK, Joyson D, Kale GB, Pappachan AL, Grover AK, et al. Development of tubular transition joints of aluminium/stainless steel by deformation diffusion bonding. *Mater Sci Technol* 2006;22(3):321–30.
- [7] Date H, Kobayakawa S, Naka M. Microstructure and bonding strength of impact-welded aluminum-stainless steel joints. *J Mater Process Technol* 1999;85:166–70.

- [8] Coelho RS, Kostka A, dos Santos JF, Pyzalla AR. EBSD technique visualization of material flow in aluminum to steel friction-stir dissimilar welding. *Adv Eng Mater* 2008;10(12):1127–33.
- [9] Derry CG, Robson JD. Characterisation and modelling of toughness in 6013-T6 aerospace aluminium alloy friction stir welds. *Mater Sci Eng A* 2008;490:328–34.
- [10] Yokoyama T. Impact performance of friction welded butt joints between 6061-T6 aluminium alloy and type 304 stainless steel. *Mater Sci Technol* 2003;19:1418–26.
- [11] Lee W-B, Schmuecker M, Mercardo UA, Biallas G, Jung S-B. Interfacial reaction in steel–aluminum joints made by friction stir welding. *Scripta Mater* 2006;55:355–8.
- [12] Kawano T, Inoue Y, Matsui M, Nishio K. Properties of aluminum alloy/stainless steel clad material produced via vacuum roll bonding. *Welding in the World* 1998;41:88–96.
- [13] Nezhad MSA, Ardakani AH. A study of joint quality of aluminum and low carbon steel strips by warm rolling. *Mater Design* 2009;30:1103–9.
- [14] Yang L, Hosoda N, Suga T. TEM investigation of the stainless steel/aluminum interface created by the surface activated bonding method. *Nucl Instr Method Phys Res B* 1997;121:519–23.
- [15] Huang Y, Ridley N, Humphreys FJ, Cui JZ. Diffusion bonding of superplastic 7075 alloy. *Mater Sci Eng* 1999;A266:295–302.
- [16] Takagi H, Maeda R, Chung TR, Hosoda N, Suga T. Effect of surface roughness on room-temperature wafer bonding by Ar beam surface activation. *Jpn J Appl Phys* 1998;37(7):4197–203.
- [17] Pregelj A, Breclj F. TiG-plasma brazed vacuum joints. *Vacuum* 1990;40:65–6.
- [18] Howlader MMR, Okada H, Kim TH, Itoh T, Suga T. Wafer level surface activated bonding tools for MEMS packaging. *J Electrochem Soc* 2004;151(7):G461–7.
- [19] Saji N, Nagai S, Tsuchiya K, Asakura H, Obata M. Development of a compact laminar flow heat exchange with stainless steel micro-tubes. *Physica C* 2001;354:148–51.